European Journal of Oral Sciences

Eur J Oral Sci 2018; 126: 345–358
DOI: 10.1111/eos.12559

European Journal of Oral Sciences

Dose- and time-dependent effects of triethylene glycol dimethacrylate on the proteome of human THP-1 monocytes

Bo W. Nilsen[1], Jaione Simon-Santamaria[2], Ulf Örtengren[1,3], Einar Jensen[4], Jack-Ansgar Bruun[2], Vibeke B. Michelsen[5], Karen K. Sørensen[2]

[1]Department of Clinical Dentistry, UiT – The Arctic University of Norway, Tromsø; [2]Department of Medical Biology, UiT – The Arctic University of Norway, Tromsø, Norway; [3]Department of Cariology, Institute of Odontology/Sahlgrenska Academy, Göteborg, Sweden; [4]Department of Pharmacy, UiT The Arctic University of Norway, Tromsø; [5]Department of Clinical Dentistry, University of Bergen, Bergen, Norway

Nilsen BW, Simon-Santamaria J, Örtengren U, Jensen E, Bruun J-A, Michelsen VB, Sørensen KK. Dose- and time-dependent effects of triethylene glycol dimethacrylate on the proteome of human THP-1 monocytes.
Eur J Oral Sci 2018; 126: 345–358. © 2018 The Authors. Eur J Oral Sci published by John Wiley & Sons Ltd

Triethylene glycol dimethacrylate (TEGDMA) is commonly used in polymer resin-based dental materials. This study investigated the molecular mechanisms of TEGDMA toxicity by identifying its time- and dose-dependent effects on the proteome of human THP-1 monocytes. The effects of different concentrations (0.07–5 mM) and exposure times (0–72 h) of TEGDMA on cell viability, proliferation, and morphology were determined using a real-time viability assay, automated cell counting, and electron microscopy, and laid the fundament for choice of exposure scenarios in the proteomic experiments. Solvents were not used, as TEGDMA is soluble in cell culture medium (determined by photon correlation spectroscopy). Cells were metabolically labeled [using the stable isotope labeled amino acids in cell culture (SILAC) strategy], and exposed to 0, 0.3 or 2.5 mM TEGDMA for 6 or 16 h before liquid chromatography-tandem mass spectrometry (LC-MS/MS) analyses. Regulated proteins were analyzed in the STRING database. Cells exposed to 0.3 mM TEGDMA showed increased viability and time-dependent upregulation of proteins associated with stress/oxidative stress, autophagy, and cytoprotective functions. Cells exposed to 2.5 mM TEGDMA showed diminished viability and a protein expression profile associated with oxidative stress, DNA damage, mitochondrial dysfunction, and cell cycle inhibition. Altered expression of immune genes was observed in both groups. The study provides novel knowledge about TEGDMA toxicity at the proteomic level. Of note, even low doses of TEGDMA induced a substantial cellular response.

Bo W. Nilsen, Department of Clinical Dentistry, University of Tromsø (UiT) – The Arctic University of Norway, Hansine Hansens veg 18, 9037 Tromsø, Norway

E-mail: bo.w.nilsen@uit.no

Key words: isotope labeling; proteomics; reactive oxygen species; tandem mass spectroscopy; triethylene glycol dimethacrylate

[The copyright line for this article was changed on 24 September 2018 after original online publication.]

Accepted for publication June 2018

Methacrylates are the most abundant organic component in polymer resin-based dental materials (PRMs). Patients and dental personnel are exposed to these substances through inhalation of volatile and particle-bound methacrylates (1–3), or by direct contact with uncured PRMs, for example, during pulp-capping procedures or handling (4, 5). In addition, elution of unreacted methacrylates from PRMs may result in exposure of patients to such substances (6, 7).

Exposure to methacrylates can induce allergic reactions (5). The ability of these compounds to react with nucleophilic centers of proteins, lipids, and/or DNA may also cause cytotoxic and/or genotoxic effects (5, 8, 9). Even though adverse reactions caused by PRMs are seldom reported, it does not imply that such substances are innocuous (10). By charting the mechanisms that underlie methacrylate toxicity, one may better understand the hazards posed by these substances (11).

Triethylene glycol dimethacrylate (TEGDMA) is a commonly used and much-studied methacrylate in dentistry (12). It has been shown in vitro to induce dose-dependent effects, such as apoptosis, cell cycle delay, and genotoxicity (12). While the toxic potency of methacrylates varies, some common modes of action have been reported, for example, induction of oxidative stress (12). The increased oxidative stress caused by TEGDMA and other methacrylates is partly attributed to depletion of scavengers of reactive oxygen species (ROS) – especially glutathione (13–15). However, increased levels of ROS may also be attributed to damage to, and subsequent dysfunction of, ROS-producing organelles, such as the endoplasmic reticulum and mitochondria (16–18). Triethylene glycol dimethacrylate is shown to modulate transcripts associated with redox-sensitive pathways, for example, nuclear factor (erythroid-derived 2)-like 2 (NRF2)-regulated pathways (19). Still, other mechanisms may be important in

TEGDMA toxicity as antioxidants are not able to nullify all the negative effects of TEGDMA and other methacrylates (20–22).

Analysis of changes in the cell proteome can give novel insight into the collective protein expression that orchestrates biological events. To our knowledge, this is the first study utilizing a proteomic approach to study the mechanisms of methacrylate toxicity. Stable isotope labeled amino acids in cell culture (SILAC) is a powerful, unbiased, and versatile metabolic-labeling strategy that is used to study differential expression of proteins using mass spectrometry (MS)-based quantitative proteomics (23). The high sensitivity of this technique makes it suitable for studies of the biological effects of TEGDMA at concentrations that previously have been described or regarded as non-toxic (24).

In this study, we aimed to explore time- and dose-dependent proteomic alterations caused by TEGDMA in human THP1 monocytes, a commonly used cell model in methacrylate toxicity studies. We initially established a non-cytotoxic and a cytotoxic concentration of TEGDMA, then performed proteomic analyses of THP-1 cells cultivated in SILAC medium, 6 and 16 h after exposure to these non-cytotoxic and cytotoxic concentrations of TEGDMA. Our study increases, and reinforces, the current understanding of how TEGDMA interacts with cells. Interestingly, even low doses of TEGDMA induced a substantial cellular response.

Material and methods

A summary of the methods is presented in Fig. 1.

Chemicals and materials

Triethylene glycol dimethacrylate (cat. no. 759406), and Triton X-100 were purchased from Sigma–Aldrich (St Louis, MO, USA). RPMI-1640 medium (supplemented with L-glutamine and sodium bicarbonate), fetal bovine serum (FBS), SILAC Protein Quantitation Kit (LysC) RPMI 1640, L-Arginine-$^{13}C_6$ hydrochloride for SILAC, NuPage 4–12% gels and buffers, and SimplyBlue SafeStain were from Thermo Fisher Scientific (Waltham, MA, USA). RealTime-Glo MT Cell Viability Assay was from Promega (Promega, Madison, WI, USA), and MycoAlert Mycoplasma Detection Kit was from Lonza (Basel, Switzerland).

Cell culture

The human monocytic cell line THP-1 (ATCC TIB-202; LOT: 59598936) was acquired from ATCC (Manassas, VA, USA). The cells were cultured in RPMI-1640 with 10% FBS, without antibiotics, at 37°C in an atmosphere of 20% O_2 and 5% CO_2, and passaged every 2–3 d at a concentration of 0.2×10^6 cells ml^{-1}. Experiments were performed with cells up to passage 26. The cell cultures were regularly screened for mycoplasma infection.

Measurement of TEGDMA solubility in cell culture medium

Solvents can interfere with the cytotoxicity of methacrylates (28). Still, there is no consensus on the type or concentration of solvent used in cell culture experiments (24). We therefore tested whether solvents could be omitted. The particle size distribution of 10 mM TEGDMA in RPMI-1640 medium was determined by photon correlation spectroscopy using a submicron particle sizer (Model 370; Nicomp, Santa Barbara, CA, USA). According to this method, a particle intensity of approximately 250–350 kHz should be achieved for valid measurement of particles in the solution (values below this indicate a solution). The value measured for 10 mM TEGDMA was 14 kHz. Therefore, TEGDMA was dissolved directly in the cell medium for all experiments.

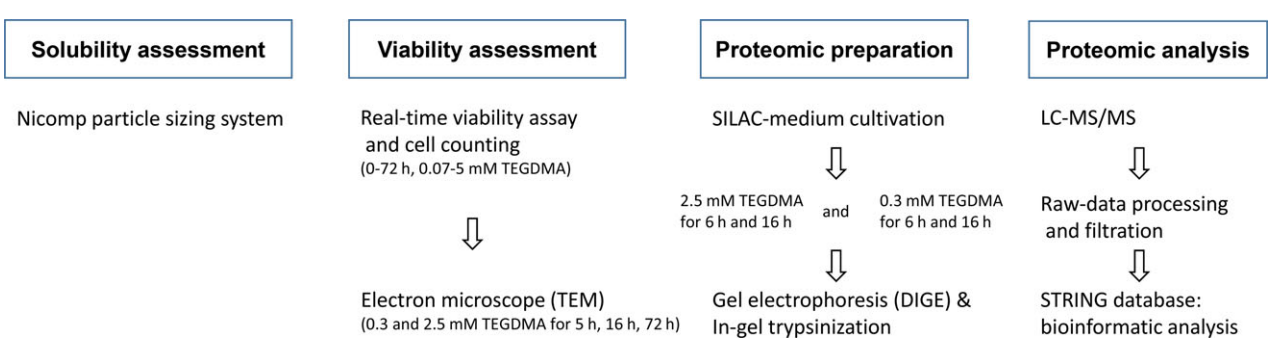

Fig. 1. Workflow summary. Solubility testing of triethylene glycol dimethacrylate (TEGDMA) was performed to examine the need for solvent. The effect of TEGDMA on viability of THP-1 cells was assessed with a real-time assay measuring cell-reduction potential and automated cell counting to define the appropriate concentrations of TEGDMA for the proteomic experiments. Transmission electron microscopy (TEM) was used to examine ultrastructural changes at the same concentrations of TEGDMA used in the proteomic experiments. THP-1 cells were cultured using the stable isotope labeled amino acids in cell culture (SILAC) strategy for metabolic incorporation of either light (^{12}C6) or heavy (^{13}C6) lysine and arginine for eight cell doublings before exposure to either 0.3 or 2.5 mM TEGDMA for 6 or 16 h. Protein expression was evaluated in comparison to untreated cells. Protein samples were subjected to gel electrophoresis [specifically, difference gel electrophoresis (DIGE)], trypsin treatment, and liquid chromatography–tandem mass spectroscopy (LC-MS/MS) analysis of tryptic peptides of mixed samples. The MaxQuant quantitative proteomic software package (25) was used to analyze the raw data, and Perseus was used for the statistical validation of proteins (26). Further bioinformatic analysis was performed with the STRING database tool set (27).

Cell viability

Cell viability was determined using the RealTime-Glo MT Cell Viability Assay (Promega), measuring the reduction potential as a marker of cell metabolism. In the present study, this assay was used in the continuous read format to determine the effect of different concentrations of TEGDMA on cell viability at different times over the course of 72 h, compared with cells not treated with TEGDMA.

Triethylene glycol dimethacrylate was weighed under sterile conditions and diluted to a 10 mM solution in RPMI-1640/10% FBS. Initially, serial dilutions of the TEGDMA solutions (5, 2.5, 1.25, 0.65, 0.3, 0.15 mM) were pipetted into white 96-well plates. Based on the results, 5 mM TEGDMA was excluded from further platings and 0.07 mM TEGDMA was used. The positive assay control was 5% Triton X-100. Cells (0.2×10^6 ml^{-1}, 50 μl) in RPMI-1640/10% FBS, 2 × RT substrate, and Nanoluc enzymes were added to all treatments, except the treatment blank, according to the manufacturer's protocol. The cells were incubated for 15 min at 37°C before the first reading was performed in a prewarmed (37°C) CLARIOstar plate reader (BMG LABTECH, Offenburg, Germany), and monitored frequently for up to 72 h.

Morphological assessment and cell counting

To supplement the cell-viability assay, cell proliferation was assessed using automated cell counting, and cell morphology was assessed by transmission electron microscopy (TEM). For cell counting, 24-well tissue-culture plates were prepared with 0.2–0.3 million THP-1 cells per well in 1 ml of RPMI-1640/10% FBS supplemented with the following concentrations of TEGDMA: 2.5, 1.25, 0.6, 0.3, 0.15, or 0.0 mM. Every 24 h for up to 72 h, the cell cultures were evaluated by phase-contrast microscopy, and the numbers of cells in aliquots of cell culture were counted in a Sysmex XP-300 Automated Hematology Analyzer (Sysmex, Kobe, Japan).

THP-1 cells for TEM were collected from cell suspensions in RPMI-1640/10% FBS medium for SILAC, then fixed in 4% formaldehyde and 2.5% glutaraldehyde in 0.1 M PHEM buffer (1 | 0.1 M PHEM, pH 7, contains 18.14 g PIPES, 6.5 g HEPES, 3.8 EGTA, 0.99 g $MgSO_4$ per l, adjusted to pH 7 with 10 M KOH), pH 7. The fixed cells were processed according to a modified version of a protocol given previously (29). The cells were post-fixed for 1 h in 0.5% glutaraldehyde in 0.1 M PHEM buffer with 0.05% malachite green. The cells were spun down, washed 2 × 15 min in 0.1 M PHEM buffer, further fixed for 1 h in 0.8% $K_3Fe(CN)_6$ and 1% OsO_4 in 0.1 M PHEM buffer, washed 2 × 15 min in 0.1 M PHEM buffer, treated for 30 min with 1% tannic acid in double-distilled water, washed 2 × 15 min in 0.1 M PHEM buffer, 2 × 3 min in double-distilled water, then incubated in 1% uranyl acetate in double-distilled water, washed 2 × 3 min in double-distilled water, and dehydrated through a graded series of ethanol (1 × 5 min 30%, 1 × 5 min 60%, 1 × 5 min 90%, 2 × 5 min 100%). Dehydrated cell pellets were infiltrated over night with 50% propylenoxide and 50% Agar 100 resin (Agar Scientific, Stansted, UK) before infiltration with 100% AGAR 100 resin overnight and polymerized at 60°C overnight. All steps, except polymerization, were carried out at room temperature, with cells in 1.5 ml Eppendorf tubes. Washing was static, and all liquid volumes were 1 ml. Ultrathin sections (70–90 nm) were analyzed using a JEM-1010 microscope (JEOL, Tokyo, Japan), equipped with a Morada CCD camera (Olympus, Tokyo, Japan).

Stable isotope labeling by amino acids in cell culture

THP-1 cells were metabolically labeled by cultivation in RPMI-1640/10% FBS medium for SILAC and prepared according to the SILAC Protein Quantitation Kit protocol (Thermo Fisher Scientific). The cells were cultured in SILAC medium containing either light ($^{12}C_6$) or heavy ($^{13}C_6$) isotope arginine and lysine, for eight cell doublings, before exposure to TEGDMA. Pilot experiments showed that six doublings yielded unsatisfactory incorporation of amino acids.

SILAC: processing of TEGDMA-treated cells

Cells with incorporation of either heavy or light amino acids were exposed for 6 or 16 h to 0.3 or 2.5 mM TEGDMA, respectively. The control was non-treated cells. Experimental state and stable isotope labels were swapped to account for systematic errors caused by metabolic incorporation of the heavy and light amino acid (label-swap).

Cell numbers were counted before mixing to ensure a 1:1 mix of ^{12}C- and ^{13}C-labeled cells. Culture media were discarded and cells were washed three times with PBS in order to process only intracellular proteins from intact cells. Cells were lysed in NuPAGE LDS Sample Buffer (4×) and stored at −70°C until gel preparation.

The samples were denatured for 30 min at 95°C and protein concentration was measured using the Millipore Direct detect protein chip. Around 50 μg of protein per sample was loaded onto a Novex gel with NuPAGE buffer and run at 200 V for 20 min, before fixation for 60 min in 40% methanol, 10% acetic acid, and 50% Milli-Q water. Proteins were visualized with SimplyBlue SafeStain and each sample were cut in three pieces for proteomics analysis.

Liquid chromatography–tandem mass spectroscopy

Gel pieces were subjected to in-gel reduction, alkylation, and tryptic digestion using 6 ng μl^{-1} of trypsin (V511A; Promega) (30). OMIX C18 tips (Varian, Palo Alto, CA, USA) were used for sample cleanup and concentration. Peptide mixtures containing 0.1% formic acid were loaded onto a Thermo Fisher Scientific EASY-nLC1000 system and EASY-Spray column (C18, particle size: 2 μm, pore size 100 Å, diameter: 75 μm, length 50 cm). Peptides were fractionated using a linear 2–100% acetonitrile gradient in 0.1% formic acid over 200 min at a flow rate of 200 nl min^{-1}. The separated peptides were analyzed using a Thermo Scientific Q-Exactive mass spectrometer. Data were collected in data-dependent mode using a top10 method.

SILAC quantitation

Raw files from the Q-Exactive MS were analyzed using the quantitative proteomics software MAXQUANT (version 1.5.6.0) (25). The SILAC pairs were quantitated in MAXQUANT, and proteins were identified using the built-in

Andromeda search engine from the Uniprot Homo sapiens (Human) database (Nov 2016). Main search peptide tolerance was set to 4.5 ppm and MS/MS mass tolerance to 20 ppm. A false discovery rate (FDR) ratio of 0.01 was needed to give protein identification. At least two peptides had to be quantitated to give a quantitation value.

Statistical validation of protein regulation was performed using the PERSEUS 1.5.6.0 software (26). To determine significant outliers a significance B test was performed. This was carried out according to the Benjamini–Hochberg procedure with an FDR of 0.05. A protein that was significantly regulated in at least two of four replicates according to the significant B-test was determined as significant regulated. Proteins that had less than two-fold change in protein levels compared with the control had to be significantly regulated in both the ^{12}C- and the ^{13}C-labeled cells, in each treatment group, to be included in further analysis.

Data analysis and statistics

Proteins that passed the initial screening process were analyzed in the STRING database (27). STRING is a database of known and predicted protein–protein interactions; for example, direct (physical) and indirect (functional) associations, based on computational prediction; read-across from different organisms; and interactions collected in other primary databases. Searches in the database were based on proteins determined regulated in the proteomic experiments. Gene ontology analysis of biological processes (hereby referred to as GO enrichment analysis) was conducted for the 0.3 and 2.5 mM TEGDMA treatment groups at both 6 and 16 h.

Graphing and statistical analysis were performed in SIGMAPLOT 13 (Systat, San Jose, CA, USA). Results from the cell-viability and cell-proliferation assays were analyzed using one-way ANOVA ($\alpha = 0.05$). Post-hoc tests were performed using the Holm–Šidák method ($\alpha = 0.05$).

Nomenclature

Proteins are referred to with their entry name in the STRING database [corresponding to Human Genome Organisation (HUGO) gene names]. Gene symbols are italicized.

Data availability

The data sets generated and analyzed during the study are available in the PRoteomics IDEntifications (PRIDE) database (31). Data are available via ProteomeXchange with identifier PXD009206.

Results

Effect of TEGDMA on THP-1 cell viability

Triethylene glycol dimethacrylate showed a time- and dose-dependent effect on THP-1 cell viability, as determined by monitoring the cellular reduction potential (Fig. 2). Incubation with ≤0.6 mM TEGDMA for 10 h increased the cell-reducing potential above the value obtained for untreated control cells, while

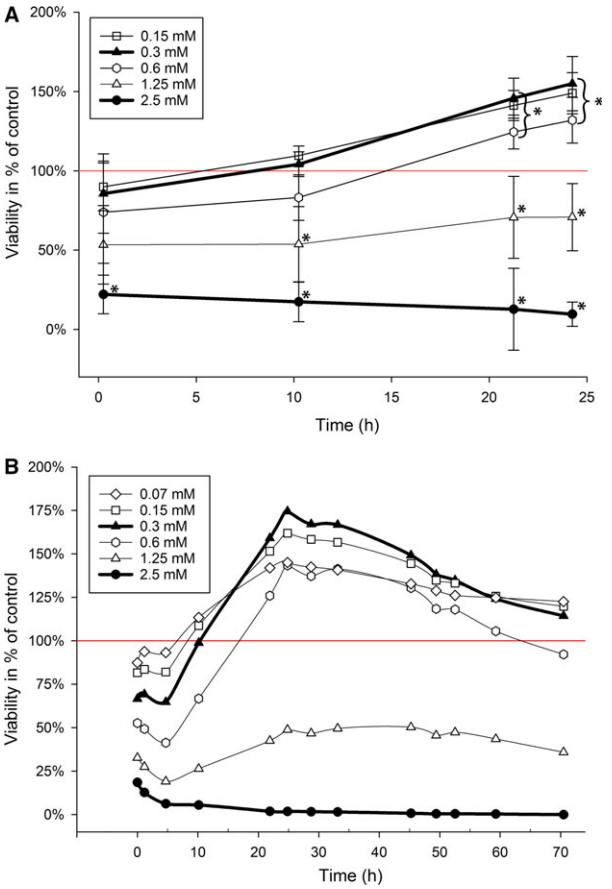

Fig. 2. Effect of triethylene glycol dimethacrylate (TEGDMA) on cell viability. THP-1 cell viability was measured using the Real-time Glo viability assay, which measures the cell-reduction potential, as described in the Material and methods. The first reading was performed 15 min after treatments were added to the cells. (A) The combined results of three independent experiments. Only common reading time points and doses from the individual experiments are shown. The horizontal line represents viability of non-TEGDMA-treated cells (control), and results are presented in percent of control value. *Statistically significant difference from the non-TEGDMA-treated control, (B) The graph shows one of the experiments in A, with all readings included. The same curve trends were observed in the two other experiments.

incubation with ≥1.25 mM TEGDMA decreased this variable.

A marked reduction in the rate of cell proliferation was apparent in cultures treated with 1.25 or 2.5 mM TEGDMA (Fig. 3). For all treatment groups, the cells appeared intact after 24 h, but after 48 and 72 h, dead or dying cells were observed in cultures treated with 2.5 mM TEGDMA (phase contrast microscopy, data not shown). Transmission electron microscopy showed that THP-1 cells exposed to 2.5 mM TEGDMA for 16 h had membrane protrusions with a more rounded shape than the membrane protrusions of untreated control cells and cells exposed to 0.3 mM TEGDMA (Fig. 4). After 72 h, all cells exposed to 2.5 mM TEGDMA were necrotic, whereas cells exposed to 0.3 mM TEGDMA looked intact and similar to those of the control group (Fig. 4).

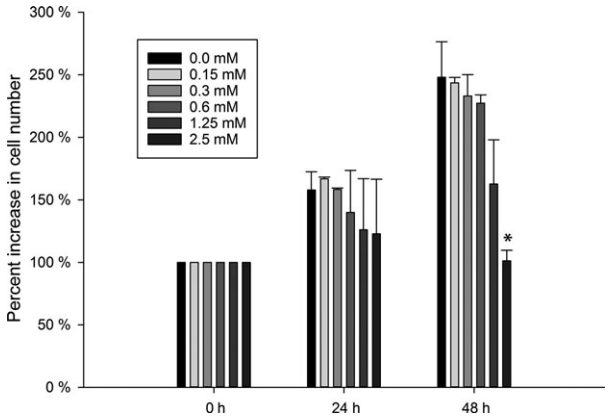

Fig. 3. Effect of triethylene glycol dimethacrylate (TEGDMA) on rate of cell proliferation. Cell numbers in THP-1 monocyte cultures exposed to different concentrations of TEGDMA for 48 h. Cell numbers were measured at the indicated time points using an automated cell counter. Cell number per well at the start of the experiment was set as 100%. The data shown are the average result of two independent cell experiments. Error bars show SD. *Statistically significant difference from the non-TEGDMA-treated control.

Proteome response to TEGDMA exposure

The objective of the proteomic study was to explore early events in THP-1 cells exposed to non-cytotoxic and cytotoxic doses of TEGDMA. Based on the results of the cell viability and proliferation studies, we chose to perform SILAC-based quantitative proteomic analyses of cells treated for 6 and 16 h with either 0.3 or 2.5 mM TEGDMA. The analyses demonstrated that 22 proteins were upregulated and 11 proteins were downregulated in cells exposed to 0.3 mM TEGDMA. In cells exposed to 2.5 mM TEGDMA, 15 proteins were upregulated and 37 proteins were downregulated. Tables 1 and 2 show an overview of dose- and time-dependent changes in the expression of individual proteins. Of note, more than 50% of the regulated proteins were significantly up- or downregulated in at least three out of four biological replicates (the inclusion criteria being two out of four). The most common reason for not identifying a protein in a replicate as regulated, was that the protein was not identified (NaN – not quantified protein), which is an inherent method weakness. One of the replicates in the 2.5 mM/6 h group was excluded from the analysis because of a very large ratio distribution compared with the other samples.

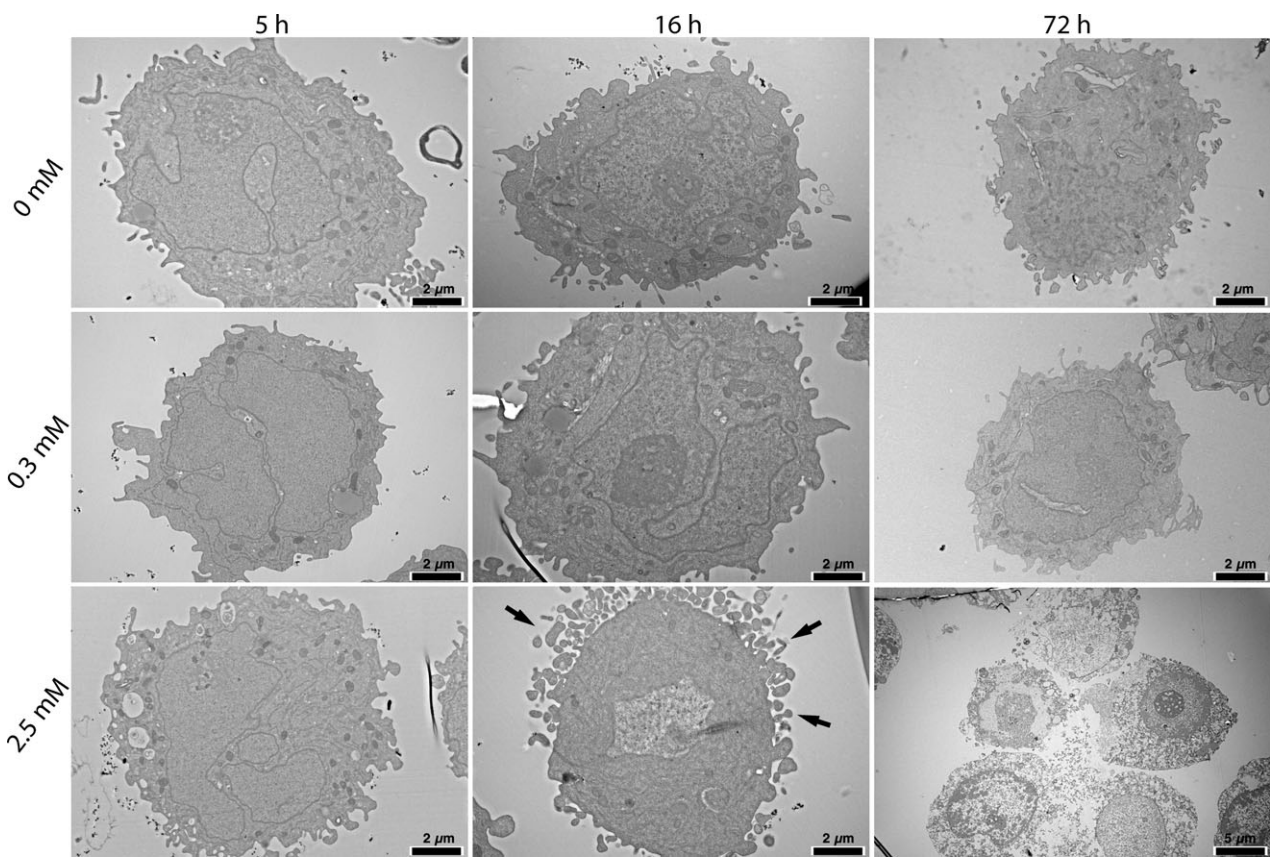

Fig. 4. Effect of triethylene glycol dimethacrylate (TEGDMA) on cell morphology. Transmission electron microscopy images of resin-embedded THP-1 monocytes exposed to TEGDMA for 5, 16, or 72 h is shown. Cells treated with 2.5 mM TEGDMA showed more rounded membrane protrusions (arrows) at 16 h than control cells and cells treated with 0.3 mM TEGDMA. After 72 h, all cells exposed to 2.5 mM TEGDMA were necrotic, whereas cells exposed to 0.3 mM TEGDMA were intact and similar to control cells. Scale bars: 2 μm, except 2.5 mM, 72 h: 5 μm.

Table 1

List of proteins found to be upregulated in THP-1 cells exposed to triethylene glycol dimethacrylate (TEGDMA)

String entry	6 h – 0.3 mM	16 h – 0.3 mM	6 h – 2.5 mM	16 h – 2.5 mM	Protein name
ABCC1		1.4			Multidrug resistance-associated protein 1
ASF1A		1.4			Histone chaperone ASF1A
CREG1		1.5			Protein CREG1
DNAJA1				1.3	DnaJ homolog subfamily A member 1
DNAJB1			1.5	3.0	DnaJ homolog subfamily B member 1
FDFT1			1.3		Squalene synthase
FERMT3		1.2			Fermitin family homolog 3
FTH1		2.1		2.4	Ferritin heavy chain; Ferritin heavy chain, N-terminally processed; Ferritin
FTL	1.2	1.4		1.6	Ferritin light chain
GCLM	1.3	2.3		1.6	Glutamate–cysteine ligase regulatory subunit
GSR		1.4			Glutathione reductase, mitochondrial
GYG1				4.8	Glycogenin-1
HMOX1	8.1	10.3	5.2	14.9	Heme oxygenase 1
HSPA1B;HSPA1A		1.3	1.9	4.9	Heat shock 70 kDa protein 1B; Heat shock 70 kDa protein 1A
HSPH1		1.1		1.5	Heat-shock protein 105 kDa
HTATIP2		1.3			Oxidoreductase HTATIP2
IDI1			1.2		Isopentenyl-diphosphate Delta-isomerase 1
MAFG					Transcription factor MafG
MAP1B		1.5			Microtubule-associated protein 1B; MAP1B heavy chain; MAP1 light chain LC1
NLRX1			4	3.6	NLR family member X1
NQO1		1.7			NAD(P)H dehydrogenase [quinone] 1
PGD		1.3			6-phosphogluconate dehydrogenase, decarboxylating
PIR		1.4			Pirin
PLIN2	1.2	2.0			Perilipin-2
PML				1.4	Protein PML
PSAT1		1.2			Phosphoserine aminotransferase
SLC3A2		1.3			4F2 cell-surface antigen heavy chain
SQSTM1		2.2			Sequestosome-1
SRXN1		3.0		3.3	Sulfiredoxin-1
TXNRD1		1.3			Thioredoxin reductase 1, cytoplasmic
UTS2				1.4	Urotensin-2
Total # proteins	4	22	6	13	

Numbers indicate average fold upregulation compared with control. Values are only shown for proteins that were significantly upregulated in at least two replicates, as described in the Material and methods.

To determine the biological significance of the regulated proteins, the results were analyzed using the STRING database. The biological relationships currently recognized between proteins are displayed in Figs 5 and 6. The GO enrichment analysis showed that six pathways were affected by 0.3 mM TEGDMA (Table 3). Among these, response to stress and oxidative stress were the pathways with the largest number of regulated proteins (16 and six proteins, respectively). Upregulation of proteins involved in oxidative stress resistance was most pronounced in cells exposed to 0.3 mM TEGDMA. In the 2.5 mM TEGDMA group, the GO enrichment analysis identified five and 13 pathways at 6 and 16 h, respectively (Table 3). At 6 h, these included regulation of protein ubiquitination, the mitotic cell cycle, and cell-cycle checkpoints; all pathways unique for the 2.5 mM treatment group. At 16 h, pathways related to apoptotic signaling, regulation of response to stress, and cellular homeostasis, as well as cellular responses to DNA-damage stimulus, were affected (Table 3) (27).

The protein-protein interaction (PPI) enrichment *P*-values for the data sets were 0.00195 (6 h) and 4.02e-05 (16 h) for the 2.5 mM exposure groups, and 0.0412 (6 h) and 5.55e-16 (16 h) for the 0.3 mM exposure groups. This indicates that the proteins in the data sets have more interactions among themselves than expected for a similarly sized random set of proteins. The PPI enrichment *P*-values further suggest that the proteins in the data sets were at least partially biologically connected as a group.

Discussion

The viability assessment and proteomic analysis showed several dose- and time-dependent effects of TEGDMA not previously reported. Concentrations of $\geq$ 1.25 mM TEGDMA caused a decrease in cell viability and

Table 2

List of proteins found to be downregulated in THP-1 cells exposed to triethylene glycol dimethacrylate (TEGDMA)

String entry	6 h – 0.3 mM	16 h – 0.3 mM	6 h – 2.5 mM	16 h – 2.5 mM	Protein name
ALDH1L2			1.8		Mitochondrial 10-formyltetrahydrofolate dehydrogenase
AZU1		1.3			Azurocidin
BRAT1			1.8		BRCA1-associated ATM activator 1
CD70			2.1		CD70 antigen
CDC20			1.6		Cell division cycle protein 20 homolog
CENPF			2.2		Centromere protein F
CEP350			1.8		Centrosome-associated protein 350
CHI3L1		1.3	1.4		Chitinase-3-like protein 1
COIL				2.6	Coilin
CTSG		1.6		1.9	Cathepsin G
DLD			1.5	1.7	Dihydrolipoyl dehydrogenase,
DNAAF5				1.8	Dynein assembly factor 5, axonemal
DNM1L				1.8	Dynamin-1-like protein
ELANE		1.5		1.8	Neutrophil elastase
FABP5		1.2			Fatty acid-binding protein, epidermal
FANCI				3.5	Fanconi anemia group I protein
GOLGA2			1.5		Golgin subfamily A member 2
GOLGB1			2.0		Golgin subfamily B member 1
IPO4				1.5	Importin-4
IRF8		1.7		4.8	Interferon regulatory factor 8
LYZ		1.6		1.5	Lysozyme C; Lysozyme
MKI67			1.4		Antigen KI-67
NCAPD3				2.4	Condensin-2 complex subunit D3
PCM1			2.2	4.0	Pericentriolar material 1 protein
PGP		1.3	1.6		Phosphoglycolate phosphatase
PRTN3		1.6		1.8	Myeloblastin
PSME1			1.5		Proteasome activator complex subunit 1
PSME2			1.5		Proteasome activator complex subunit 2
PSME3				1.6	Proteasome activator complex subunit 3
RIF1				1.8	Telomere-associated protein RIF1
RTN3		1.4			Reticulon
SAMHD1				1.2	Deoxynucleoside triphosphate triphosphohydrolase
SYNE3			1.6		Nesprin-3
TK1			2.0		Thymidine kinase, cytosolic; Thymidine kinase
TMEM173				2.6	Stimulator of interferon genes protein
TONSL				2.7	Tonsoku-like protein
TRMT1		1.8			tRNA (guanine(26)-N(2))-dimethyltransferase
TXNRD1			1.4		Thioredoxin reductase 1, cytoplasmic
TYMS				2.4	Thymidylate synthase
VIM			1.4		Vimentin
ZMYM3				2.5	Zinc finger MYM-type protein 3
Total # proteins	0	11	19	20	

Numbers indicate average fold downregulation compared with control. Values are only shown for proteins that were significantly downregulated in at least two replicates, as described in the Material and methods.

inhibition of cell proliferation, whereas concentrations of TEGDMA below 0.6 mM increased cell viability without affecting cell proliferation (Figs 2 and 3). This corresponded to the effects of TEGDMA observed at the cell proteomic level. Expression of proteins associated with oxidative stress, in particular proteins reported to be controlled by the redox-sensitive transcription factor, NRF2, were altered in both treatment groups.

Nuclear factor (erythroid-derived 2)-like 2 is referred to as 'the master regulator of the antioxidant response' (32) and initiates the transcription of genes related to neutralization of ROS (32, 33). Nuclear factor (erythroid-derived 2)-like 2 also controls expression of other stress-related factors, such as detoxification enzymes, proteasomes, and heat-shock proteins (33). Altered levels of proteins associated with NRF2 activity have been observed in cells exposed to hydroxyethyl methacrylate (HEMA) (34–36), bisphenol A diglycidyl ether dimethacrylate (Bis-GMA) (37), and urethane dimethacrylate (UDMA) (38), and upregulation of NRF-2 associated factors is suggested to be a general protective mechanism in cells exposed to methacrylates (36).

Heme oxygenase 1 (HMOX1) was the protein most strongly upregulated in the present proteomic data set, independent of concentration or time of exposure of the THP-1 cells to TEGDMA. Heme oxygenase 1 is an established NFR2-regulated protein and a key enzyme in the cellular response to oxidative stress (39). Heme

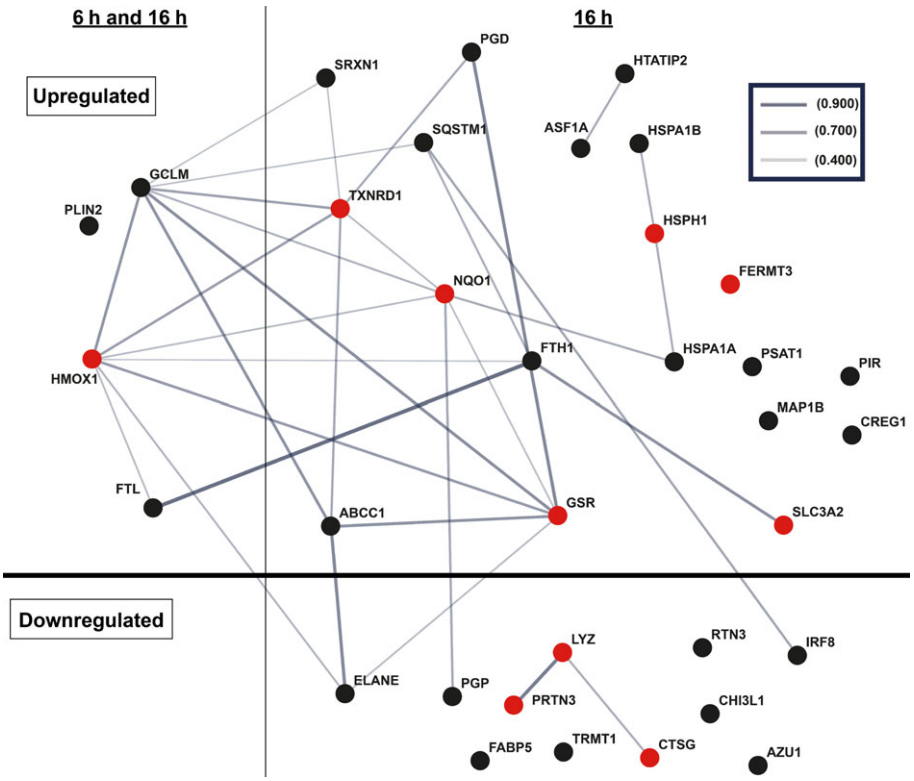

Fig. 5. Confidence of association between regulated proteins in THP-1 cells after exposure to 0.3 mM triethylene glycol dimethacrylate (TEGDMA) for 6 and 16 h (compared to non-treated control cells). Circles (red and black) represent regulated proteins. Lines between circles represent protein–protein associations, that is, shared function, as indicated by the analysis performed using the String database tool (27). A red circle indicates that this protein belongs to the Gene Ontology biological process of Response to stress (GO0006950). Box: line boldness between proteins indicates strength of confidence of the associations as shown in the STRING analyses. The full protein name of each abbreviation can be found in Table 1 or 2.

oxygenase 1 mediates the first step in heme catabolism by cleaving free heme to Fe(II), carbon monoxide, and biliverdin (39). The Fe(II) generated can promote the Fenton reaction, resulting in the conversion of H_2O_2 into OH radicals. However, the concomitant regulation of iron-binding proteins, such as ferritin heavy chain 1 (FTH1) and ferritin light chain (FTL), promotes detoxification of the Fe(II) ion and subsequent storage of iron (40). In our study, upregulation of FTH1 and FTL were displayed in both the 0.3 mM and 2.5 mM TEGDMA treatment groups (Table 1).

Heme oxygenase 1 is thought to act as a cytoprotectant, both directly, by reducing the amount of cytotoxic free heme (which increases during oxidative stress), and indirectly through the production of carbon monoxide and biliverdin (39). Biliverdin is converted to the antioxidant bilirubin, which is suggested to have protective effects on cell-membrane components, analogous to how glutathione protects cytoplasmic components (40). Upregulation of HMOX-1 has previously been reported at the mRNA level, in dental pulp cells exposed to TEGDMA (19, 41, 42). Upregulation of HMOX-1 is also reported in cells exposed to UDMA, HEMA, and Bis-GMA (34–38). Heme oxygenase 1 (and subsequent iron sequestration) is therefore likely to play an important role in maintaining the redox balance in cells exposed to methacrylates.

Cells exposed to ≤0.6 mM TEGDMA showed increased viability compared with non-TEGDMA-treated control cells, suggesting an increased metabolic rate. This is in accordance with the enhanced metabolism observed in mouse fibroblasts (3T3 cells) exposed to 0.5 mM TEGDMA (43), which was suggested by the authors to be caused by upregulation of detoxification processes. Changes in proteins associated with metabolic processes were also observed in our proteomic data, as 6-phosphogluconate dehydrogenase (PGD), a component of the pentose phosphate pathway, was upregulated by 0.3 mM TEGDMA. The pentose phosphate pathway is a major source for reductive power in the cells through the generation of NADPH (44). The availability of NADPH might explain some of the dose-dependent differences in the expression of regulated antioxidants proteins between treatment groups.

Antioxidant pathways are important for maintaining homeostatic ROS levels. The three main pathways for removal of ROS involve thioredoxins, catalases, and glutathione – all of which are regulated by NRF2 activity (32, 45). Glutatione is the most abundant intracellular ROS scavenger (33), and a key determinant of the redox status of the cell. In the present study, TEGDMA affected antioxidant pathways in a dose-dependent manner, with upregulation of proteins

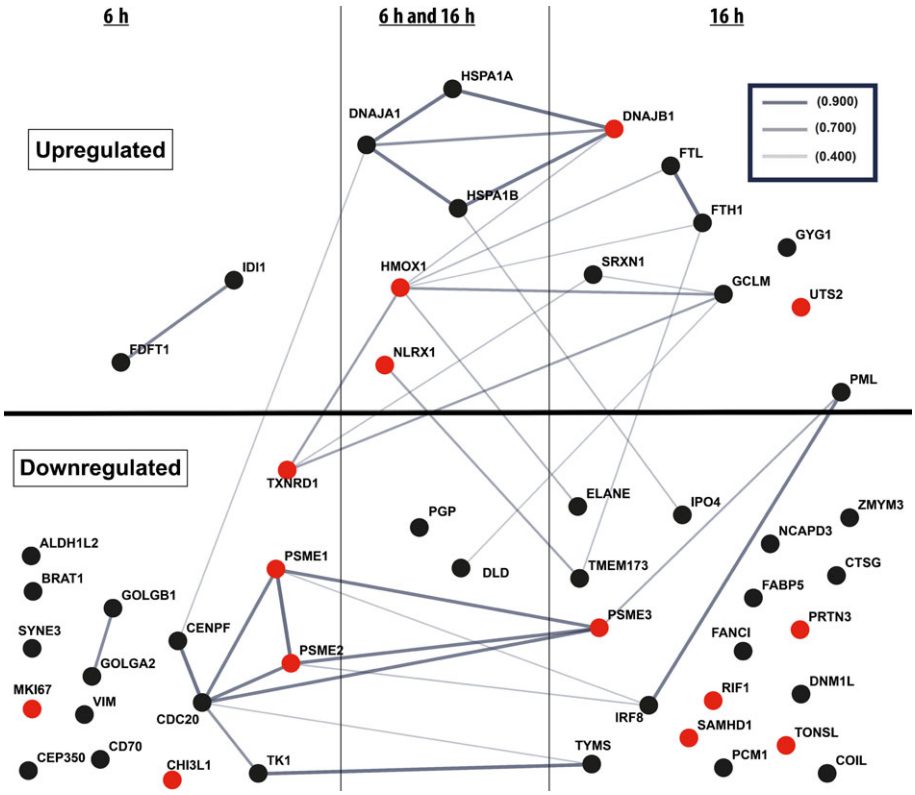

Fig. 6. Confidence of association between regulated proteins in THP-1 cells after exposure to 2.5 mM triethylene glycol dimethacrylate (TEGDMA) for 6 and/or 16 h (compared to non-treated control cells). Circles (red and black) represent regulated proteins. Lines between circles represent protein-protein associations, that is, shared function, as indicated by the analysis performed with the String database tool (27). A red circle indicates that this protein belongs to the Gene Ontology biological process of Response to stress (GO0006950). Box: line boldness between proteins indicates strength of confidence of the associations as shown in the STRING analyses. The full protein name of each abbreviation can be found in Table 1 or 2.

involved in glutathione homeostasis being most pronounced in the low-dose group. The first rate-limiting enzyme of glutathione synthesis, glutamate-cysteine ligase regulatory subunit (GCLM), was upregulated at both time points by 0.3 mM TEGDMA, and only at 16 h by 2.5 mM TEGDMA. Increased glutathione synthesis was indicated in the low-TEGDMA-dose group by upregulation of phosphoserine aminotransferase 1 (PSAT1), an enzyme involved in production of glycine, a substrate for glutathione synthesis (46). Upregulation of glutathione reductase (GSR), which catalyzes the recovery of glutathione by reducing glutathione disulfide, was also only seen for the low-TEGDMA-dose group.

Triethylene glycol dimethacrylate is suggested to cause depletion of glutathione, without creation of glutathione disulfide, by forming TEGDMA–glutathione adducts at concentrations of TEGDMA above 0.5 mM (47). This may explain the difference in GSR expression between cells exposed to 0.3 and 2.5 mM TEGDMA, as formation of adducts at high doses of TEGDMA would prevent upregulation of GSR (17, 47). Furthermore, the low reduction potential seen in THP-1 cells after treatment with 2.5 mM TEGDMA suggests the presence of low levels of NADPH, which is the substrate for GSR (48). Differences in TEGDMA–glutathione adduct formation and levels of NADPH may also explain why thioredoxin reductase 1 (TXNRD1) was downregulated by 2.5 mM TEGDMA but upregulated by 0.3 mM TEGDMA. Thioredoxin reductase 1 represents a class of redox proteins that facilitates the reduction of other proteins by cysteine thiol-disulfide exchange by NADPH (49, 50). Increased levels of reduced thioredoxin have been associated with increased cell survival through nuclear factor-kappaB (NF-κB) signaling (49).

Our results also show that a recently discovered member of the oxidoreductase family, sulfiredoxin 1 (SRXN1) (51), is upregulated by both low and high concentrations of TEGDMA. This is in line with findings in a study on human fibroblasts in which upregulation of *SRXN1* was shown to occur at transcriptional level after exposure to TEGDMA (41). Sulfiredoxin 1 is thought to act as a bridge between multiple redox systems by catalyzing the reduction of cysteine-sulfinic acid, formed under exposure to oxidants (51). Taken together with our findings, this suggests that sulfiredoxin and thioredoxin activities are important in counteracting TEGDMA toxicity.

In our data set, TEGDMA increased the production of heat-shock proteins, of which expression is reported to be partially controlled by NRF2 (33). Heat-shock proteins are normally expressed at low levels under physiological conditions and are upregulated by cellular

Table 3

Gene ontology enrichment analysis of biological processes that were affected in THP-1 cells exposed to 0.3 mM (A) or 2.5 mM (B, C) triethylene glycol dimethacrylate (TEGDMA) for 6 or 16 h

(A) 0.3 mM (16 h) #Pathway ID	Pathway description	Matching proteins
GO.0044130	Negative regulation of growth of symbiont in host	CTSG, ELANE, IRF8, **SQSTM1**
GO.0045073	Regulation of chemokine biosynthetic process	AZU1, ELANE, **HMOX1**
GO.0006950	Response to stress	**ASF1A**, AZU1, CHI3L1, CTSG, FABP5, **FERMT3**, **GSR**, **HMOX1**, **HSPH1**, LYZ, **NQO1**, PRTN3, **SLC3A2**, **SQSTM1**, **SRXN1**, **TXNRD1**
GO.0006979	Response to oxidative stress	**GCLM**, **GSR**, **HMOX1**, **NQO1**, **SRXN1**, **TXNRD1**
GO.0042742	Defense response to bacterium	AZU1, CTSG, ELANE, IRF8, LYZ
GO.0070943	Neutrophil-mediated killing of symbiont cell	CTSG, ELANE

(B) 2.5 mM (6 h) #Pathway ID	Pathway description	Matching proteins
GO.0031397	Negative regulation of protein ubiquitination	CDC20, CENPF, **DNAJA1**, PSME1, PSME2
GO.0051436	Negative regulation of ubiquitin-protein ligase activity involved in mitotic cell cycle	CDC20, CENPF, PSME1, PSME2
GO.0051348	Negative regulation of transferase activity	CDC20, CENPF, **DNAJA1**, PSME1, PSME2
GO.1901991	Negative regulation of mitotic cell cycle phase transition	CDC20, CENPF, PSME1, PSME2
GO.0007093	Mitotic cell cycle checkpoint	CDC20, CENPF, PSME1, PSME2

(C) 2.5 mM (16 h) #Pathway ID	Pathway description	Matching proteins
GO.0043901	Negative regulation of multi-organism process	CTSG, ELANE, IRF8, **NLRX1**, **PML**
GO.0044130	Negative regulation of growth of symbiont in host	CTSG, ELANE, IRF8
GO.2001236	Regulation of extrinsic apoptotic signaling pathway	**GCLM**, **HMOX1**, PCM1, **PML**, PSME3
GO.0033993	Response to lipid	CTSG, ELANE, **HMOX1**, IRF8, PCM1, **PML**, TYMS, **UTS2**
GO.0070943	Neutrophil-mediated killing of symbiont cell	CTSG, ELANE
GO.0050776	Regulation of immune response	CTSG, ELANE, **HMOX1**, **NLRX1**, **PML**, PSME3, SAMHD1, TMEM173
GO.0006875	Cellular metal ion homeostasis	ELANE, **FTH1**, **FTL**, **HMOX1**, **PML**, **UTS2**
GO.0080134	Regulation of response to stress	**DNAJA1**, **DNAJB1**, DNM1L, ELANE, **NLRX1**, **PML**, PSME3, RIF1, SAMHD1, TMEM173
GO.2001233	Regulation of apoptotic signaling pathway	DNM1L, **GCLM**, **HMOX1**, PCM1, **PML**, PSME3
GO.0006950	Response to stress	CTSG, **DNAJB1**, FAPB5, FANCI, **HMOX1**, **NLRX1**, PCM1, PRTN3, PSME3, RIF1, SAMHD1, **SRXN1**, TMEM173, TONSL, **UTS2**
GO.0019725	Cellular homeostasis	DLD, ELANE, **FTH1**, **FTL**, **HMOX1**, **PML**, **UTS2**
GO.0006974	Cellular response to DNA damage stimulus	**DNAJA1**, FANCI, **HMOX1**, **PML**, PSME3, RIF1, TONSL
GO.0043900	Regulation of multi-organism process	CTSG, ELANE, IRF8, **NLRX1**, **PML**, TMEM173

Bold, upregulated; underlined, downregulated.

stress, such as increased oxidation of biomolecules or protein misfolding (33). Induction of heat-shock proteins by TEGDMA was dose- and time-dependent, with the highest levels recorded after exposure to 2.5 mM TEGDMA (Table 1). This was probably a result of pronounced changes in the cell redox balance and subsequent oxidative damage to biomolecules. In the 2.5 mM TEGDMA treatment group, components of the ubiquitin–proteasome system were downregulated already at 6 h, suggesting an early, pronounced oxidative insult (52).

Triethylene glycol dimethacrylate has previously been reported to increase levels of biomarkers of ROS-induced DNA-damage, such as 8-oxoG adducts and ataxia-telangiectasia kinase (ATM) (53). In our analysis, early signs of oxidized base damage were indicated in THP-1 cells treated with 0.3 mM TEGDMA by upregulation of the anti-silencing function protein 1A (ASF1A) and HIV-1 Tat interactive protein 2 (HTATIP2; CC3), which are associated with genotoxic stress (54). However, 0.3 mM TEGDMA did not affect THP-1 cell growth negatively. In the 2.5 mM TEGDMA treatment group, cell growth was markedly impaired. There also was a marked downregulation of thymidylate synthetase (TYMS), an enzyme involved in the synthesis of an essential precursor for DNA synthesis. Inhibition of this protein is linked to DNA strand breakage, cell-growth inhibition, and cell death (55).

The growth arrest and proteomic alterations that were observed in cells exposed to 2.5 mM TEGDMA suggest damage of nuclear DNA. As mitochondrial DNA (mtDNA) is three- to sevenfold more

susceptible to oxidative damage than nuclear DNA (56), damage to mtDNA is likely to occur. Mitochondrial DNA damage negatively influences mitochondrial membrane potential and production of ATP- and NADPH, while increasing production of ROS as a result of reduced expression of crucial mitochondrial proteins (18, 56, 57). In the present study, mitochondrial dysfunction was suggested in the real-time viability assay by the decreased reduction potential observed in cells exposed to ≥1.25 mM TEGDMA. Early mitochondrial dysfunction was also indicated by the downregulation of mitochondrial enzymes involved in energy metabolism, such as dihydrolipoamide dehydrogenase (DLD) in the high-dose TEGDMA group. In addition, the decreased expression of aldehyde dehydrogenase 1 family member L2 (ALDH1L2) suggests increased cell susceptibility to ROS, as this protein is known to be a crucial protector against oxidative stress in the mitochondria (58). Finally, the lowered levels of BRAT1 induced by exposure to 2.5 mM TEGDMA may be associated with metabolic abnormalities that ultimately lead to mitochondrial malfunction, loss of redox balance, and cell death (59).

Declining ATP levels and compromised redox balance as a result of mitochondrial damage are common causes of regulated cell death (60). Triethylene glycol dimethacrylate has previously been demonstrated to cause apoptosis through the intrinsic and extrinsic pathways (61). In the GO enrichment analysis, extrinsic apoptotic signaling pathways were advocated for the group treated with 2.5 mM TEGDMA. Moreover, the mitochondrial NLR family member X1 (NLRX1) was among the most upregulated proteins in this group. This protein is suggested to control the balance between extrinsic and intrinsic apoptotic signaling pathways by interacting with the electron transport chain (62).

Interestingly, TEGDMA affected the expression of proteins associated with immune functions in the THP-1 monocyte. Several of the regulated proteins in both dose groups are associated with immune functions linked to pathogen clearance and inflammation (Table 3). The influence of TEGDMA on immune functions could be related to NRF2 activity (63); for example, anti-inflammatory effects induced in THP-1 cells have been reported to be mediated by an HMOX-1/NRF2 cascade (63, 64). Interferon regulatory factor 8 (IRF8), a protein described to be essential for immune responses (65), was downregulated by both 0.3 and 2.5 mM TEGDMA, although downregulated to a greater degree in the high-dose-TEGDMA group. Macrophages deficient in IRF8 have decreased autophagic activity (65).

Autophagy is an essential cell process, partly controlled by NRF2 (66), that promotes cell survival by removing dysfunctional organelles and proteins. For example, defective or damaged mitochondria caused by exposure to TEGDMA will contribute to ROS formation if not removed (17, 67). A previous study, utilizing TEM, reported that TEGDMA did not induce autophagy in human gingival fibroblasts (68). However, our proteomic data gave some indication of the induction of autophagic processes by TEGDMA. For example, sequestosome-1 (SQSTM1) (67), cellular repressor of E1A-stimulated genes (CREG1) (69), and microtubule-associated protein 1B (MAP1B) were upregulated in the 0.3 mM TEGDMA group. Upregulation of MAP1B has been linked to membrane blebbing and autophagic vesicle formation (70). Autophagic vacuole formation was also observed in THP-1 cells by TEM in our study, although with no clear difference between the treated groups and controls. The more evident autophagic protein response in the low-dose-TEGDMA group may be a result of the fact that high concentrations of TEGDMA inhibit the phosphoinositide 3-kinase (PI3K) pathway (71), which has a crucial role in autophagy (72).

Low doses of TEGDMA (0.3 mM) caused upregulation of proteins associated with increased cell survival, such as NAD(P)H dehydrogenase [quinone] (NQO1). The NRF2-regulated protein, NQO1, controls several functions linked to increased cell survival (73, 74), such as reduction in the levels of intracellular quinonoids through consumption of NADPH, thus preventing the formation of free radicals (semiquinones) and ROS (73, 74). Another cytoprotective protein upregulated in the low-dose group was the multidrug resistance-associated protein 1 (ABCC1). This protein mediates ATP-dependent transport of glutathione and glutathione conjugates, as well as xenobiotics, across the plasma membrane (75). In relation to TEGDMA toxicity, ABCC1 may be necessary to avoid accumulation of intracellular TEGDMA and/or TEGDMA-glutathione adducts (75). Active transport of TEGDMA, together with cellular metabolism, may explain why intracellular concentrations of TEGDMA are only a fraction of the extracellular available concentration (28, 76).

To sum up, the proteomic alterations displayed in human THP-1 monocytes exposed to TEGDMA showed increased oxidative stress responses at early time points, regardless of dose. The highest dose of TEGDMA (2.5 mM) caused changes in proteins associated with cell cycle arrest and apoptotic pathways. Of note, concentations of TEGDMA previously referred to as non-toxic caused proteomic changes that may alter the cell phenotype and immune function, and increase cell survival through mechanisms that involve antioxidant pathways. As exposure to a concentration of TEGDMA lower than 0.3 mM increased cell viability in a similar manner as 0.3 mM TEGDMA, one may speculate if the cell proteome will be affected by exposure to even lower doses of TEGDMA.

In light of the present and reported findings on cellular effects of TEGDMA, direct exposure to uncured or insufficiently cured materials containing TEGDMA should be avoided. This is particularly relevant for dental materials containing TEGDMA (and other methacrylates) that are indicated for direct application on living tissue such as resin-modified pulp-capping materials (77). Furthermore, indirect contact with

methacrylates through adhesives during bonding, where similar concentrations as used in our experiments can be reached (78, 79), may alter the homeostasis of exposed cells. In occupational settings, dental personnel may be repeatedly exposed to low doses of TEGDMA and other methacrylates (3). It has been speculated whether chronic activation of antioxidant pathways, such as NRF2, may cause an indiscriminate, favorable environment for cell survival that may, over time, lead to transformation of cells (80–82). Epigenetic effects of TEGDMA – and other methacrylates – can therefore be an interesting area for further studies.

In conclusion, the present study adds new data and reinforces the current understanding concerning the interaction of methacrylates with cells. Of note, a low, apparently non-toxic dose of TEGDMA caused early alteration in the proteome of exposed cells. Low-dose effects of methacrylates may therefore be important from a health hazard perspective.

Acknowledgements – We thank Randi Olsen and Augusta Hlin Aspar at the Advanced Microscopy Core Facility at UiT – The Arctic University of Norway, Tromsø, for skilled assistance in preparation of samples for electron microscopy. We also thank Dr. Natasa Skalko-Basnet at the Department of Pharmacy, UiT, for help with solubility measurements of TEGDMA. This work was supported by a grant from the Norwegian Directorate of Health to Ulf Ørtengren (14/1493). The funding source had no influence on the work.

Conflict of interest – None.

References

1. Marquardt W, Seiss M, Hickel R, Reichl FX. Volatile methacrylates in dental practices. *J Adhes Dent* 2009; **11**: 101–107.
2. Cokic SM, Duca RC, Godderis L, Hoet PH, Seo JW, Van Meerbeek B, Van Landuyt KL. Release of monomers from composite dust. *J Dent* 2017; **60**: 56–62.
3. Henriks-Eckerman ML, Alanko K, Jolanki R, Kerosuo H, Kanerva L. Exposure to airborne methacrylates and natural rubber latex allergens in dental clinics. *J Environ Monit* 2001; **3**: 302–305.
4. Nilsen BW, Jensen E, Örtengren U, Michelsen VB. Analysis of organic components in resin-modified pulp capping materials: critical considerations. *Eur J Oral Sci* 2017; **125**: 183–194.
5. Wallenhammar LM, Örtengren U, Andreasson H, Barregård L, Björkner B, Karlsson S, Wrangsjö K, Meding B. Contact allergy and hand eczema in Swedish dentists. *Contact Dermatitis* 2000; **43**: 192–199.
6. Van Landuyt KL, Nawrot T, Geebelen B, De Munck J, Snauwaert J, Yoshihara K, Scheers H, Godderis L, Hoet P, Van Meerbeek B. How much do resin-based dental materials release? A meta-analytical approach *Dent Mater* 2011; **27**: 723–747.
7. Michelsen VB, Kopperud HBM, Lygre GB, Björkman L, Jensen E, Kleven IS, Svahn J, Lygre H. Detection and quantification of monomers in unstimulated whole saliva after treatment with resin-based composite fillings in vivo. *Eur J Oral Sci* 2012; **120**: 89–95.
8. Ginzkey C, Zinnitsch S, Steussloff G, Koehler C, Hackenberg S, Hagen R, Kleinsasser NH, Froelich K. Assessment of HEMA and TEGDMA induced DNA damage by multiple genotoxicological endpoints in human lymphocytes. *Dent Mater* 2015; **31**: 865–876.
9. Blaschke U, Eismann K, Böhme A, Paschke A, Schüürmann G. Structural alerts for the excess toxicity of acrylates, methacrylates, and propiolates derived from their short-term and long-term bacterial toxicity. *Chem Res Toxicol* 2012; **25**: 170–180.
10. Schedle A, Örtengren U, Eidler N, Gabauer M, Hensten A. Do adverse effects of dental materials exist? What are the consequences, and how can they be diagnosed and treated? *Clin Oral Implants Res* 2007; **18**: 232–256.
11. Hartung T, McBride M. Food for Thought... on mapping the human toxome. *Altex* 2011; **28**: 83–93.
12. Schweikl H, Spagnuolo G, Schmalz G. Genetic and cellular toxicology of dental resin monomers. *J Dent Res* 2006; **85**: 870–877.
13. Noda M, Wataha JC, Lewis JB, Kaga M, Lockwood PE, Messer RLW, Sano H. Dental adhesive compounds alter glutathione levels but not glutathione redox balance in human THP-1 monocytic cells. *J Biomed Mater Res B Appl Biomater* 2005; **73B**: 308–314.
14. Nocca G, Callà C, Martorana GE, Cicillini L, Rengo S, Lupi A, Cordaro M, Luisa Gozzo M, Spagnuolo G. Effects of dental methacrylates on oxygen consumption and redox status of human pulp cells. *Biomed Res Int* 2014; **2014**: 956579.
15. Ansteinsson V, Kopperud HB, Morisbak E, Samuelsen JT. Cell toxicity of methacrylate monomers-the role of glutathione adduct formation. *J Biomed Mater Res A* 2013; **101**: 3504–3510.
16. Malhotra JD, Kaufman RJ. Endoplasmic reticulum stress and oxidative stress: a vicious cycle or a double-edged sword? *Antioxid Redox Signal* 2007; **9**: 2277–2293.
17. Lefeuvre M, Amjaad W, Goldberg M, Stanislawski L. TEGDMA induces mitochondrial damage and oxidative stress in human gingival fibroblasts. *Biomaterials* 2005; **26**: 5130–5137.
18. Van Houten B, Woshner V, Santos JH. Role of mitochondrial DNA in toxic responses to oxidative stress. *DNA Repair (Amst)* 2006; **5**: 145–152.
19. Schweikl H, Hiller K-A, Eckhardt A, Bolay C, Spagnuolo G, Stempfl T, Schmalz G. Differential gene expression involved in oxidative stress response caused by triethylene glycol dimethacrylate. *Biomaterials* 2008; **29**: 1377–1387.
20. Martins CA, Leyhausen G, Geurtsen W, Volk J. Intracellular glutathione: a main factor in TEGDMA-induced cytotoxicity? *Dent Mater* 2012; **28**: 442–448.
21. Stanislawski L, Lefeuvre M, Bourd K, Soheili-Majd E, Goldberg M, Périanin A. TEGDMA-induced toxicity in human fibroblasts is associated with early and drastic glutathione depletion with subsequent production of oxygen reactive species. *J Biomed Mater Res A* 2003; **66**: 476–482.
22. Ansteinsson V, Solhaug A, Samuelsen JT, Holme JA, Dahl JE. DNA-damage, cell-cycle arrest and apoptosis induced in BEAS-2B cells by 2-hydroxyethyl methacrylate (HEMA). *Mutat Res* 2011; **723**: 158–164.
23. Ong SEE, Foster LJ, Mann M. Mass spectrometric-based approaches in quantitative proteomics. *Methods* 2003; **29**: 124–130.
24. Nilsen BW, Örtengren U, Simon-Santamaria J, Sørensen KK, Michelsen VB. Methods and terminology used in cell-culture studies of low-dose effects of matrix constituents of polymer resin-based dental materials. *Eur J Oral Sci* 2016; **124**: 511–525.
25. Cox J, Mann M. MaxQuant enables high peptide identification rates, individualized p.p.b.-range mass accuracies and proteome-wide protein quantification. *Nat Biotechnol* 2008; **26**: 1367–1372.
26. Tyanova S, Temu T, Sinitcyn P, Carlson A, Hein MY, Geiger T, Mann M, Cox J. The Perseus computational platform for comprehensive analysis of (prote)omics data. *Nat Methods* 2016; **13**: 731–740.
27. Szklarczyk D, Franceschini A, Wyder S, Forslund K, Heller D, Huerta-Cepas J, Simonovic M, Roth A, Santos A, Tsafou KP, Kuhn M, Bork P, Jensen LJ, Von Mering C.

STRING v10: protein-protein interaction networks, integrated over the tree of life. *Nucleic Acids Res* 2015; **43**: D447–D452.
28. Nocca G, D'Antò V, Rivieccio V, Schweikl H, Amato M, Rengo S, Lupi A, Spagnuolo G, Ant VD. Effects of ethanol and dimethyl sulfoxide on solubility and cytotoxicity of the resin monomer triethylene glycol dimethacrylate. *J Biomed Mater Res B Appl Biomater* 2012; **100B**: 1500–1506.
29. Cocchiaro J, Kumar Y, Fischer ER, Hackstadt T, Valdivia RH. Cytoplasmic lipid droplets are translocated into the lumen of the Chlamydia trachomatis parasitophorous vacuole. *Proc Natl Acad Sci U S A* 2008; **105**: 9379–9384.
30. Shevchenko A, Wilm M, Vorm O, Mann M. Mass spectrometric sequencing of proteins silver-stained polyacrylamide gels. *Anal Chem* 1996; **68**: 850–858.
31. Vizcaíno JA, Csordas A, Del-Toro N, Dianes JA, Griss J, Lavidas I, Mayer G, Perez-Riverol Y, Reisinger F, Ternent T, Xu QW, Wang R, Hermjakob H. 2016 update of the PRIDE database and its related tools. *Nucleic Acids Res* 2016; **44**: D447–D456.
32. Nguyen T, Nioi P, Pickett CB. The Nrf2-antioxidant response element signaling pathway and its activation by oxidative stress. *J Biol Chem* 2009; **284**: 13291–13295.
33. Trachootham D, Lu W, Ogasawara MA, Nilsa R-DV, Huang P. Redox regulation of cell survival. *Antioxid Redox Signal* 2008; **10**: 1343–1374.
34. Schweikl H, Widbiller M, Krifka S, Klement J, Petzel C, Bolay C, Hiller KA, Buchalla W. Interaction between LPS and a dental resin monomer on cell viability in mouse macrophages. *Dent Mater* 2016; **32**: 1492–1503.
35. Krifka S, Hiller KA, Spagnuolo G, Jewett A, Schmalz G, Schweikl H. The influence of glutathione on redox regulation by antioxidant proteins and apoptosis in macrophages exposed to 2-hydroxyethyl methacrylate (HEMA). *Biomaterials* 2012; **33**: 5177–5186.
36. Gallorini M, Petzel C, Bolay C, Hiller KA, Cataldi A, Buchalla W, Krifka S, Schweikl H. Activation of the Nrf2-regulated antioxidant cell response inhibits HEMA-induced oxidative stress and supports cell viability. *Biomaterials* 2015; **56**: 114–128.
37. Chang M-C, Chen L-I, Chan C-P, Lee J-J, Wang T-M, Yang T-T, Lin P-S, Lin H-J, Chang H-H, Jeng J-H. The role of reactive oxygen species and hemeoxygenase-1 expression in the cytotoxicity, cell cycle alteration and apoptosis of dental pulp cells induced by BisGMA. *Biomaterials* 2010; **31**: 8164–8171.
38. Chang HH, Chang MC, Wang HH, Huang GF, Lee YL, Wang YL, Chan CP, Yeung SY, Tseng SK, Jeng JH. Urethane dimethacrylate induces cytotoxicity and regulates cyclooxygenase-2, hemeoxygenase and carboxylesterase expression in human dental pulp cells. *Acta Biomater* 2014; **10**: 722–731.
39. Gozzelino R, Jeney V, Soares MP. Mechanisms of cell protection by heme oxygenase-1. *Annu Rev Pharmacol Toxicol* 2010; **50**: 323–354.
40. Baranano DE, Rao M, Ferris CD, Snyder SH. Biliverdin reductase: a major physiologic cytoprotectant. *Proc Natl Acad Sci U S A* 2002; **99**: 16093–16098.
41. Cho SG, Lee JW, Heo JS, Kim SY. Gene expression change in human dental pulp cells exposed to a low-level toxic concentration of triethylene glycol dimethacrylate: an RNA-seq analysis. *Basic Clin Pharmacol Toxicol* 2014; **115**: 282–290.
42. Öncel Torun Z, Torun D, Demirkaya K, Yavuz ST, Sarper M, Avcu F. Hypoxia inhibits mineralization ability of human dental pulp cells treated with TEGDMA but increases cell survival in accordance with the culture time. *Arch Oral Biol* 2016; **71**: 59–64.
43. Engelmann J, Leyhausen G, Leibfritz D, Geurtsen W. Metabolic effects of dental resin components in vitro detected by NMR spectroscopy. *J Dent Res* 2001; **80**: 869–875.
44. Xu SN, Wang TS, Li X, Wang YP. SIRT2 activates G6PD to enhance NADPH production and promote leukaemia cell proliferation. *Sci Rep* 2016; **6**: 1–13.
45. Gorrini C, Harris IS, Mak TW. Modulation of oxidative stress as an anticancer strategy. *Nat Rev Drug Discov* 2013; **12**: 931–947.
46. DeNicola GM, Chen P-H, Mullarky E, Sudderth JA, Hu Z, Wu D, Tang H, Xie Y, Asara JM, Huffman KE, Wistuba II, Minna JD, DeBerardinis RJ, Cantley LC. NRF2 regulates serine biosynthesis in non–small cell lung cancer. *Nat Genet* 2015; **47**: 1475–1481.
47. Binderman I, Bahar H, Zeligson S, Amariglio N, Rechavi G, Shoham S, Yaffe A. TEGDMA modulates glutathione transferase P1 activity in gingival fibroblast. *J Dent Res* 2007; **83**: 914–919.
48. Yin F, Sancheti H, Cadenas E. Mitochondrial thiols in the regulation of cell death pathways. *Antioxid Redox Signal* 2012; **17**: 1714–1727.
49. Matthews JR, Wakasugi N, Virelizier JL, Yodoi J, Hay RT. Thioredoxin regulates the DNA binding activity of NF-kappa B by reduction of a disulphide bond involving cysteine 62. *Nucleic Acids Res* 1992; **20**: 3821–3830.
50. Circu ML, Aw TY. Reactive oxygen species, cellular redox systems, and apoptosis. *Free Radic Biol Med* 2010; **48**: 749–762.
51. Baek JY, Han SH, Sung SH, Lee HE, Kim YM, Noh YH, Bae SH, Rhee SG, Chang TS. Sulfiredoxin protein is critical for redox balance and survival of cells exposed to low steady-state levels of H_2O_2. *J Biol Chem* 2012; **287**: 81–89.
52. Lilienbaum A. Relationship between the proteasomal system and autophagy. *Int J Biochem Mol Biol* 2013; **4**: 1–26.
53. Eckhardt A, Gerstmayr N, Hiller K, Bolay C, Waha C, Spagnuolo G, Camargo C, Schmalz G, Schweikl H. TEGDMA-induced oxidative DNA damage and activation of ATM and MAP kinases. *Biomaterials* 2009; **30**: 2006–2014.
54. Fong S, King F, Shtivelman E. CC3/TIP30 affects DNA damage repair. *BMC Cell Biol* 2010; **11**: 23.
55. Curtin NJ, Harris AL, Aherne GW. Mechanism of cell death following thymidylate synthase inhibition: 2'-deoxyuridine-5'-triphosphate accumulation, DNA damage, and growth inhibition following exposure to CB3717 and dipyridamole. *Cancer Res* 1991; **51**: 2346–2352.
56. Yakes FM, Van Houten B. Mitochondrial DNA damage is more extensive and persists longer than nuclear DNA damage in human cells following oxidative stress. *Proc Natl Acad Sci U S A* 1997; **94**: 514–519.
57. Ballinger SW, Patterson C, Yan CN, Doan R, Burow DL, Young CG, Yakes FM, Van Houten B, Ballinger CA, Freeman BA, Runge MS. Hydrogen peroxide - and peroxynitrite-induced mitochondrial DNA damage and dysfunction in vascular endothelial and smooth muscle cells. *Circ Res* 2000; **86**: 960–966.
58. Ohta S, Ohsawa I, Kamino K, Ando F, Shimokata H. Mitochondrial ALDH2 deficiency as an oxidative stress. *Ann N Y Acad Sci* 2004; **1011**: 36–44.
59. So EY, Ouchi T. BRAT1 deficiency causes increased glucose metabolism and mitochondrial malfunction. *BMC Cancer* 2014; **14**: 548.
60. Galluzzi L, Bravo-San Pedro JM, Vitale I, Aaronson SA, Abrams JM, Adam D, Alnemri ES, Altucci L, Andrews D, Annicchiarico-Petruzzelli M, Baehrecke EH, Bazan NG, Bertrand MJ, Bianchi K, Blagosklonny MV, Blomgren K, Borner C, Bredesen DE, Brenner C, Campanella M, Candi E, Cecconi F, Chan FK, Chandel NS, Cheng EH, Chipuk JE, Cidlowski JA, Ciechanover A, Dawson TM, Dawson VL, De Laurenzi V, De Maria R, Debatin KM, Di Daniele N, Dixit VM, Dynlacht BD, El-Deiry WS, Fimia GM, Flavell RA, Fulda S, Garrido C, Gougeon ML, Green DR, Gronemeyer H, Hajnoczky G, Hardwick JM, Hengartner MO, Ichijo H, Joseph B, Jost PJ, Kaufmann T, Kepp O, Klionsky DJ, Knight RA, Kumar S, Lemasters JJ, Levine B, Linkermann A, Lipton SA, Lockshin RA, López-Otín C, Lugli E, Madeo F, Malorni W, Marine JC, Martin SJ, Martinou JC, Medema JP, Meier P, Melino S, Mizushima N, Moll U, Muñoz-Pinedo C, Nuñez G, Oberst A, Panaretakis T, Penninger JM, Peter ME, Piacentini M, Pinton P, Prehn JH, Puthalakath H, Rabinovich GA,

Ravichandran KS, Rizzuto R, Rodrigues CM, Rubinsztein DC, Rudel T, Shi Y, Simon HU, Stockwell BR, Szabadkai G, Tait SW, Tang HL, Tavernarakis N, Tsujimoto Y, Vanden Berghe T, Vandenabeele P, Villunger A, Wagner EF, Walczak H, White E, Wood WG, Yuan J, Zakeri Z, Zhivotovsky B, Melino G, Kroemer G. Essential versus accessory aspects of cell death: recommendations of the NCCD 2015. *Cell Death Differ* 2015; **22**: 58–73.

61. Batarseh G, Windsor LJ, Labban NY, Liu Y, Gregson K. Triethylene glycol dimethacrylate induction of apoptotic proteins in pulp fibroblasts. *Oper Dent* 2014; **39**: E1–E8.
62. Soares F, Tattoli I, Rahman MA, Robertson SJ, Belcheva A, Liu D, Streutker C, Winer S, Winer DA, Martin A, Philpott DJ, Arnoult D, Girardin SE. The mitochondrial protein NLRX1 controls the balance between extrinsic and intrinsic apoptosis. *J Biol Chem* 2014; **289**: 19317–19330.
63. Battino M, Giampieri F, Pistollato F, Sureda A, de Oliveira MR, Pittalà V, Fallarino F, Nabavi SF, Atanasov AG, Nabavi SM. Nrf2 as regulator of innate immunity: a molecular Swiss army knife!. *Biotechnol Adv* 2018; **36**: 358–370.
64. An YW, Jhang KA, Woo SY, Kang JL, Chong YH. Sulforaphane exerts its anti-inflammatory effect against amyloid-β peptide via STAT-1 dephosphorylation and activation of Nrf2/HO-1 cascade in human THP-1 macrophages. *Neurobiol Aging* 2016; **38**: 1–10.
65. Gupta M, Shin D-M, Ramakrishna L, Goussetis DJ, Platanias LC, Xiong H, Morse HC, Ozato K. IRF8 directs stress-induced autophagy in macrophages and promotes clearance of Listeria monocytogenes. *Nat Commun* 2015; **6**: 6379.
66. Pajares M, Jiménez-Moreno N, Dias IHK, Debelec B, Vucetic M, Fladmark KE, Basaga H, Ribaric S, Milisav I, Cuadrado A. Redox control of protein degradation. *Redox Biol* 2015; **6**: 409–420.
67. Kongara S, Karantza V. The interplay between autophagy and ROS in tumorigenesis. *Front Oncol* 2012; **2**: 1–13.
68. Teti G, Orsini G, Salvatore V, Focaroli S, Mazzotti MC, Ruggeri A, Mattioli-Belmonte M, Falconi M. HEMA but not TEGDMA induces autophagy in human gingival fibroblasts. *Front Physiol* 2015; **6**: 1–8.
69. Yan CH, Li Y, Tian XX, Zhu N, Song HX, Zhang J, Sun MY, Han YL. CREG1 ameliorates myocardial fibrosis associated with autophagy activation and Rab7 expression. *Biochim Biophys Acta* 2015; **1852**: 353–364.
70. Harrison B, Kraus M, Burch L, Stevens C, Craig A, Gordon-Weeks P, Hupp TR. DAPK-1 binding to a linear peptide motif in MAP1B stimulates autophagy and membrane blebbing. *J Biol Chem* 2008; **283**: 9999–10014.
71. Spagnuolo G, Galler K, Schmalz G, Cosentino C, Rengo S, Schweikl H. Inhibition of Phosphatidylinositol 3-Kinase Amplifies TEGDMA-induced Apoptosis in Primary Human Pulp Cells. *J Dent Res* 2004; **83**: 703–707.
72. Codogno P, Meijer AJ. Autophagy and signaling: their role in cell survival and cell death. *Cell Death Differ* 2005; **12** (Suppl 2): 1509–1518.
73. Tsvetkov P, Reuven N, Shaul Y. Ubiquitin-independent p53 proteasomal degradation. *Cell Death Differ* 2010; **17**: 103–108.
74. Nioi P, Hayes JD. Contribution of NAD(P)H:quinone oxidoreductase 1 to protection against carcinogenesis, and regulation of its gene by the Nrf2 basic-region leucine zipper and the arylhydrocarbon receptor basic helix-loop-helix transcription factors. *Mutat Res* 2004; **555**: 149–171.
75. Leslie EM, Deeley RG, Cole SPC. Toxicological relevance of the multidrug resistance protein 1, MRP1 (ABCC1) and related transporters. *Toxicology* 2001; **167**: 3–23.
76. Durner J, Walther UI, Zaspel J, Hickel R, Reichl F-XX. Metabolism of TEGDMA and HEMA in human cells. *Biomaterials* 2010; **31**: 818–823.
77. Silva GAB, Gava E, Lanza LD, Estrela C, Alves JB. Subclinical failures of direct pulp capping of human teeth by using a dentin bonding system. *J Endod* 2013; **39**: 182–189.
78. Hanks CT, Wataha JC, Parsell RR, Strawn SE, Fat JC. Permeability of biological and synthetic molecules through dentine. *J Oral Rehabil* 1994; **21**: 475–487.
79. Gerzina TM, Hume WR. Diffusion of monomers from bonding resin-resin composite combinations through dentine in vitro. *J Dent* 1994; **24**: 125–128.
80. Córdova EJ, Martínez-Hernández A, Uribe-Figueroa L, Centeno F, Morales-Marín M, Koneru H, Coleman MA, Orozco L. The NRF2-KEAP1 pathway is an early responsive gene network in arsenic exposed lymphoblastoid cells. *PLoS ONE* 2014; **9**: e88069.
81. Wang D, Ma Y, Yang X, Xu X, Zhao Y, Zhu Z, Wang X, Deng H, Li C, Gao F, Tong J, Yamanaka K, An Y. Hypermethylation of the Keap1 gene inactivates its function, promotes Nrf2 nuclear accumulation, and is involved in arsenite-induced human keratinocyte transformation. *Free Radic Biol Med* 2015; **89**: 209–219.
82. Sporn MB, Liby KT. NRF2 and cancer: the good, the bad and the importance of context. *Nat Rev Cancer* 2012; **12**: 564–571.